CREBBP/EP300 mutation is associated with poor outcome in HNSCC and targetable with synthetic cytotoxicity.

Manish Kumar PhD[1]*, David Molkentine BS[2]*, Jessica Molkentine BS[2], Kathleen Bridges MS[1], Tongxin Xie MD, PhD[3], Liangpeng Yang PhD[1], Meng Gao MBBS, PhD[3], Mitchell J. Frederick, PhD[4], Sahil Seth PhD[5], Mohamed Abdelhakiem MD[2], Faye Johnson MD, PhD[6], Jing Wang PhD[7], Li Shen MS[7], Timothy Heffernan PhD[5], Aakash Sheth BS[8], Robert Ferris MD, PhD[9], Jeffrey N. Myers MD, PhD[3], Curtis R. Pickering, PhD[3,*], Heath D. Skinner MD, PhD[2,*,#]

[1] *Department of Experimental Radiation Oncology, University of Texas, MD Anderson Cancer Center, Houston, USA.*

[2] *Department of Radiation Oncology, University of Pittsburgh, UPMC Hillman Cancer Center, Pittsburgh, USA.*

[3] *Department of Head and Neck Surgery, University of Texas, MD Anderson Cancer Center, Houston, USA.*

[4] *Department of Otolaryngology-Head & Neck Surgery, Baylor College of Medicine, Houston, USA.*

[5] *Institute for Applied Cancer Science, University of Texas, MD Anderson Cancer Center, Houston, USA.*

[6] *Department of Thoracic and Head and Neck Medical Oncology, University of Texas, MD Anderson Cancer Center, Houston, USA.*

[7] *Department of Biostatistics, University of Texas, MD Anderson Cancer Center, Houston, USA.*

[8] *Robert Wood Johnson Medical School, Rutgers University, New Brunswick, USA.*

[9] *Department of Otolaryngology, University of Pittsburgh, UPMC Hillman Cancer Center,*

Pittsburgh, USA

[*] contributed equally

 # Corresponding author:

Heath D. Skinner, MD, PhD

UPMC Hillman Cancer Center

5117 Centre Ave, Suite 2.6

Pittsburgh, PA, 15213-1862

Phone: (412) 623-3275

Email: skinnerh@upmc.edu

The authors report no conflict of interest related to this manuscript.

Abstract

Background: Head and neck squamous cell carcinoma (HNSCC) harbors few directly targetable mutations, however several mutations in this malignancy may be sensitive to synthetic cytotoxicity.

Methods: Whole exome sequencing in human HNSCC tumors (n=235) was analyzed for effect on outcome. *In vivo* shRNA screening in HNSCC models was performed following by in vitro and in vivo studies of tumor response and DNA damage repair.

Results: Mutation in either the histone acetyltransferases CREBBP and EP300 or CASP8 were associated with poor outcome following radiation therapy in HNSCC. *In vivo* shRNA screening identified synthetic cytotoxicity in CREBBP/EP300 mutant tumors by combining radiation and inhibition of histone acetyltransferase (HAT) function. This effect appears to be due to increased DNA damage following ionizing radiation through inhibition of homologous recombination and altered acetylation of histone marks.

Conclusion: CREBBP/EP300 mutation is associated with radiation resistance in HNSCC and is targetable via synthetic cytotoxicity.

Background

Outcomes for head and neck squamous cell carcinoma (HNSCC) have remained largely unchanged for the past two decades. Treatment for this malignancy generally involves radiation, alone or in combination with resection and/or cytotoxic chemotherapy. There are few biologically driven radiosensitizers and only one clinically utilized biomarker in HNSCC, the presence of the human papillomavirus (HPV). In HPV negative patients, several prognostic markers have been investigated by ourselves and others (1–5), however validation of these markers is limited.

Tumor genomic alterations can lead to increased susceptibility to a targeted therapy (synthetic lethality or synthetic cytotoxicity). The most common example of this being increased sensitivity to PARP inhibition in BRCA1 altered tumors (6). However, most large-scale screening approaches using cell lines with known genomic status have not treated with radiation and have not identified tumor mutations or alterations that can sensitize to radiation treatment (7). Genomically-driven radiosensitizers have the potential of only affecting the mutated cancer cells and not normal cells which would be a huge advantage.

Most anti-neoplastic agents tested in the pre-clinical setting ultimately fail to be translated to the clinic due to multiple factors, including the artificial nature of *in vitro* systems and unforeseen toxicity (8,9). Targets identified as radiosensitizers in an *in vitro* model, may underperform *in vivo* due to complex interactions within the tumor itself. Additionally, the same microenvironment interactions could be potential targets for radiosensitization and may not be readily identified using *in vitro* screening techniques.

In the current manuscript we coupled analysis of clinical HNSCC, identifying mutations associated with poor outcomes following radiation, with *in vivo* screening data to identify potential targets for synthetic cytotoxicity in tumors harboring these mutations.

Methods

Clinical data

This study was approved via appropriate Institutional Review Board. The initial patient cohort consisted of the HNSCC TCGA group which satisfied the following criteria: i) whole exome sequencing data is available and ii) received radiation as part of their initial therapy (Supplemental Table 1). Of the 523 patients in the TCGA cohort 276 patients met these criteria. Genes with mutations in ≥10% of tumors and significance on MutSig (TP53, FAT1, CDKN2A, NOTCH1, PIK3CA, NSD1, CREBBP and EP300 (combined due to significant homology) and CASP8) were examined (10,11). A subset (n=94) of patients from the TCGA HNSCC cohort treated with surgery and post-operative radiation with known patterns of failure was also analyzed (Supplemental Table 2). All tumors in this subset cohort were HPV/p16 negative as demonstrated by immunohistochemistry (IHC) or In-situ hybridization (ISH). Additional information available in the Supplemental methods.

Cell lines and cell culture

HNSCC cell lines (UMSCC47, UMSCC22a, UMSCC25, UMSCC1, HN31, HN30, UMSCC17b, UPCI:SCC152 and HN5) used in this study were generously supplied by Dr. Jeffrey Myers via The University of Texas MD Anderson Cancer Center Head and

Neck cell line repository. HEK-293T was purchased form American Type Culture Collection (Manassas, VA). Cell lines were tested for mycoplasma and genotyped at the MD Anderson Characterized Cell Line Core before experiments. UMSCC47 and UMSCC25 were maintained in Dulbecco modified Eagle medium (Gibco, USA), supplemented with 10% fetal bovine serum, 1% penicillin/streptomycin, 1% sodium pyruvate, 1% nonessential amino acids, and 2% vitamins. HEK-293T, HN5, HN30, HN31, UMSCC1, UMSCC17b and UMSCC22a were maintained in DMEM/F-12 50/50 medium supplemented with 10% fetal bovine serum and 1% penicillin/streptomycin. UPCI:SCC152 and FaDu were maintained in MEM medium supplemented with 10% fetal bovine serum, 1% nonessential amino acids and 1% penicillin/streptomycin. All cell lines were incubated at 37°C and 5% CO2 atmosphere.

Immunoblot analysis

Cells were washed in PBS and scraped and collected in sufficient amount of RIPA lysis buffer (50mM Tris pH 7.5, 1mM EDTA pH 8, 1% NP-40, 150mM NaCl, 10mM MgCl2, 1X protease inhibitor cocktail and 1X phosphatase inhibitor cocktail. This was mixed by vortexing and sonicated for 2 minutes at 100 amplitude with QSonica Q700 sonicator (Newton, CT) This was then centrifuged at 14,000 rpm for 15 min at 4°C. Supernatant was transferred to a fresh vial and total protein contents were estimated by Bradford reagent (Sigma) and equal amounts of proteins (50 µg/lane) were resolved on 4-15% gradient (SDS)-polyacrylamide gel (Bio-Rad). The proteins were then electro-transferred for 10 minutes onto polyvinylidene-difluoride (PVDF) membrane using Transblot Turbo device (Bio-Rad). After blocking with 5% non-fat powdered milk in Tris-buffered saline (TBS, 0.1 M, pH = 7.4), blots were incubated with primary antibody at

4°C overnight. The following primary antibodies were used: p300 (NM11) from Santa Cruz Biotechnology (Santa Cruz, CA), and CBP, H3K9, H3K18, H3K27, total Histone3 and β-actin from Cell Signaling Technology (Danvers, MA). After each step, blots were washed three times with Tween (0.1%)-Tris-buffer saline (TTBS). Goat anti-mouse and anti-rabbit secondary antibody conjugated to horseradish peroxidase ((GE Healthcare, Chicago, Illinois) were used, and signal was generated with the ECL2 western blotting substrate (Pierce Biotechnology, Rockford, IL) on HyBlot CL autoradiographic film (Thomas Scientific, Swedesboro, NJ). Protein abundance of β-actin served as a control for protein loading in each lane.

Plasmids and shRNA transfection

Cell lines were transfected with shRNAs specific for the CREBBP, EP300 gene or control scrambled shRNA via lentiviral vectors containing the puromycin resistance gene (GE Dharmacon). Lentiviral–containing shRNA CREBBP, EP300 and Control were transfected. After two days cells were subjected for antibiotic selection. Pooled knockdown cells and counterparts shControl cells were assessed for CREBBP protein expression by immunoblotting. shRNA sequences are given as follow:

shRNA CREBBP   2# TRCN0000006486   GCTATCAGAATAGGTATCATT

                          3# TRCN0000006487   GCGTTTACATAAACAAGGCAT

shRNA EP300   #2 TRCN0000039884 5`-CCAGCCTCAAACTACAATAAA-3`

                          #4 TRCN0000039886 5`-CCCGGTGAACTCTCCTATAAT-3`

                          #5 TRCN0000039887 5`-CGAGTCTTCTTTCTGACTCAA-3`

***In vivo* shRNA screening**

A loss-of-function (LOF) screen using two pooled shRNA libraries (targets in Supplemental table 3). One library targeted genes associated with DNA damage repair derived from Gene Ontology gene sets. The second library included shRNAs for genes known to be targetable by agents currently in clinical or investigational use. Pilot studies were performed to examine the frequency of tumor initiating cells (TIC) and determine whether the cell line could maintain shRNA library complexity *in vivo*. Additionally, pilot studies were performed to identify the fractionated (2 Gy/day) dose of radiation needed to achieve approximately 20% tumor reduction for each model by the conclusion of the experiment. For the experimental method itself, generally, the method of Carugo and colleagues. was used, with the addition of fractionated radiation (12). Additional details available in the Supplemental methods.

In Vitro TUNEL assay

Following experimental treatments, all cells were collected including floating cells and TUNEL staining was performed using the APO-DIRECT Kit (BD Pharmingen) according to the manufacturer's protocol. Briefly, 1 million cells were fixed in 1% paraformaldehyde on ice for 30min. Cells were then washed in PBS and fixed in 70% ethanol overnight at -20C. Cells were washed twice with provided buffer then stained with 50ul of DNA labeling solution at 37C for 45min. Cells were then rinsed twice with provided buffer and resuspended in 300ul of rinse buffer. Cells were then analyzed by flow cytometry using the BD Accuri C6 flow cytometer (BD Biosciences) with 488nm laser, 533/30 filter and FL1 detector. 10,000 events were measured per sample.

Immunohistochemical studies

Paraffin embedded sections (4µm) of mouse tumor and control irradiated tissues were collected on coated slides and was deparaffinized in xylene, hydrated along different gradients of alcohol followed by heat induced antigen retrieval in 0.01M Citrate buffer (pH 6.0). Sections were then incubated with 5% rabbit or goat serum for 60 minutes to block non-specific binding followed by incubation in rabbit polyclonal anti-CREBBP antibody 0.5 µg/ul, LSB3360, LSBio, CA) (1:400 dilution) antibody in humidified chamber overnight at 4^0C. Next day after washing twice with Tris buffered saline (TBS 0.1M, pH 7.4) the tissue sections were incubated with (0.3%) hydrogen peroxide for 20 minutes to quench the endogenous peroxidase activity. The primary antibody was detected using the universal VECTASTAIN Kit (Vectastain®, CA USA). Slides were washed with Tris-buffered saline (TBS, 0.1 M, pH = 7.4), 4 times after every step. Antigens were detected using 3, 3'-diaminobenzidine (Vectastain®, Burlingame, CA) as chromogen. Finally tissue sections were counterstained with Mayer's hematoxylin, mounted with DPX and examined under the light microscope (Leica microscope, NY, USA). Prostate cancer tissue sections were used as a positive control for CREBBP expression as described earlier. In the negative control tissue sections, isotype specific non-immune rabbit IgG replaced the primary antibody.

In vivo TUNEL assay

Paraffin embedded sections (4µm) of UMSCC47 tumor xenografts were mounted on coated slides and sent to HistoWiz Inc. (histowiz.com) for TUNEL staining and quantification. TUNEL staining was performed using a Standard Operating Procedure and fully automated workflow with Deadend colorimetric TUNEL system from Promega. After staining, sections were dehydrated and film coverslipped using a TissueTek-

Prisma and Coverslipper (Sakura). Whole slide scanning (40x) was performed on an

Aperio AT2 (Leica Biosystems). Images were analyzed using Halo (version

2.3.2089.34) image analysis software from Indica Labs (Albuquerque, NM). Regions of

interest were selected. TUNEL staining was segmented using the CytoNuclear

algorithm. Total cell counts were thresholded into low, medium, and high intensity

staining bins.

Histone Extraction

Histone proteins were extracted from treated or untreated cells using a histone

extraction kit (Abcam) according to the manufacturer's protocol. Briefly, cells were

harvested, and pellet was obtained by centrifugation at 10,000 rpm for 5 minutes at 4˚C.

The cells were re-suspended in 1X pre-lysis buffer and incubated at 4˚C for 10 minutes

on a rotator and then centrifuged for one minute at 10,000 rpm at 4˚C. The cell pellet

was re-suspended in lysis buffer at a concentration of 200 uL/10^7 cells and incubated on

ice for 30 minutes, then centrifuged at 12,000 rpm for 5 minutes at 4˚C. The supernatant

was collected and 300uL balance buffer-DTT was added per 1mL supernatant. The

quantity of protein extracted was measured with a DC protein assay kit (Bio-Rad,

Hercules, CA, USA). 2-4 µg of protein were separated by western blot analysis as

described above.

Clonogenic Survival Assay

Clonogenic survival assays were performed in order to determine the response

to radiation (sensitivity or resistance). Calculated numbers of cells were plated in 6-well

plates for 12-14 hours. The next day cells were incubated with specified drugs before

irradiating at the indicated doses. The cells were allowed to form colonies over a 10- to

14-day incubation period and then fixed in a 0.25% crystal violet in methanol solution. Numbers of colonies containing more than 50 cells each were counted to determine surviving fraction and surviving curves were generated using GraphPad Prism.

Immunofluorescence staining

Immunofluorescence was performed to measure quantitative differences in DNA damage repair and response. Cells were cultivated on cover slips placed in 35-mm cell culture dishes. At specified time points after exposure to radiation (2 Gy), cells were fixed in 4% paraformaldehyde for 15 min at room temperature on shaker, briefly washed in phosphate-buffered saline or PBS (Biorad) and placed in 70% ethanol at 4°C overnight. These fixed cells were washed with PBS twice to remove ethanol and permeabilized with 0.1% IGEPAL (octylphenoxypolyethoxyethanol) for 20 min at room temperature on shaker, followed by blocking in 2% bovine serum albumin (Sigma) for 60 min, and then incubated with anti-γH2AX (1:400), 53BP1 (1:200) or anti-BRCA1 primary antibody (1:500) overnight at 4°C. Next day cells were washed three times with PBS and incubated for 45 minutes in the dark in secondary anti-mouse antibody conjugated to FITC to visualize γH2AX or Cy3 to visualize BRCA1. Secondary anti-rabbit antibody conjugated to Cy3 was used to visualize 53BP1. DNA was stained with 4', 6-diamidino-2-phenylindole (Sigma) at 1:1000 (1 microgram/ml). Immunoreactions were visualized with a Leica Microsystems microscope (Wetzlar, Germany), and foci were counted with Image J software (https://imagej.nih.gov/ij/).

Mouse xenograft model

Male athymic nude mice (6-8 weeks old, ENVIGO/HARLAN, USA) were randomly assigned to one of 6 groups of 10 mice each: untreated UMSCC47 shControl, untreated UMSCC47 CREBBP#2 and CREBBP#3 knockdown, irradiated UMSCC47-shControl, UMSCC47 CREBBP#2 and CREBBP#3 knockdown. UMSCC47 tumor cells (2×10^6 in 0.1 mL of serum-free medium) were injected subcutaneously in the right dorsal flank of each mouse. After palpable tumors had developed, tumor diameters were measured with digital calipers, and tumor volume was calculated as A × B2 × 0.5, where A represents the largest diameter and B the smallest diameter. When the tumor volumes reached approximately ~150 mm^3, tumors were irradiated with 16 Gy (2 Gy/day x 8 days) and tracked for approximately 4 weeks. At that time the experiment was completed, and tumors harvested. Similar, experiment was performed using UMSCC22A shControl, UMSCC22A shCREBBP#2, and UMSCC22A shCREBBP#3. To compare tumor growth delay between groups, linear regression of the growth curve was calculated for each group and the slope of each curve was compared between groups using Graph Pad Prism (v8.0).

Results

Mutations in CASP8 or the CBP-p300 coactivator family (CREBBP and EP300) are associated with outcome following radiation in HNSCC.

We examined the Head and Neck TCGA cohort for patients treated with radiation (Supplemental table 1) for mutations associated with overall survival (Fig. 1A). The genes CREBBP and EP300 were combined into a single category (CBP-p300 coactivator family) because of their high genetic and functional similarity. Only 3 genes (TP53 (p=0.015), CASP8 (p=0.055) and CREBBP/EP300 (p=0.046)) were associated

with OS, as was the presence of HPV (p=0.002) (47 patients, 17.4%) (Figure 1A). Neither tumor stage (p=0.69), nodal stage (p=0.61) nor tumor site (p=0.79) were significantly associated with survival in this population, most likely due to the high proportion of advanced stages. TP53 was also associated with OS in the unirradiated patients (HR 1.52, p=0.053), while CASP8 (p=0.41) and CREBBP/EP300 (p=0.89) were, not indicating that in these two groups relationship with survival may be dependent upon radiation response.

Because the TCGA represents a heterogenously treated cohort of patients and patterns of failure are not recorded, we examined patient outcomes in a subset of 94 patients with HPV negative HNSCC treated uniformly with surgery and post-operative radiation with known patterns of failure (Supplemental table 1). In this analysis, TP53 (as a binary variable), was not associated with OS or LRR (Fig. 1B & C). Mutations in both CASP8 and the CBP-p300 coactivator family were associated with significantly higher rates of LRR in this patient population (Fig. 1A & B).

The presence of CDKN2A mutation was associated with decreased time to distant metastasis (DM) it did not achieve statistical significance (p=0.08). No other mutation examined was associated with time to distant metastasis (DM).

CREBBP, EP300 or dual specificity protein kinase (TTK) inhibition combined with radiation in CREBBP/EP300 mutated tumors leads to synthetic cytotoxicity.

We wished to identify synthetic cytotoxicity associated with CASP8 or CREBBP/EP300 mutation and performed *in vivo* shRNA library screens in tumors generated from 5 HNSCC cell lines treated with radiation (Supplemental table 3). Two

libraries were used, one of "druggable" targets and the other targeting the DNA-damage repair pathway (Supplemental Table 4).

To determine a gene level summary estimate of the impact of knock-out of each gene we performed redundant shRNA analysis (RSA) to generate log p-values for each gene for both irradiated and unirradiated tumor (Figure 2A). In the current study, the focus is primarily on the synthetic cytotoxicity in combination with radiation, thus targets preferentially associated with increased response to radiation (below and to the left of the blue dashed line in Fig. 2A) were selected for further study. The RSA log p-values and fold change for each of these targets were compared between either CASP8 wild type (wt) and mutant tumors (Fig. 2B) or CREBBP/EP300 wt and mutant tumors (Fig. 2C). While no differences were observed in the comparison of CASP8 wt and mutant tumors, several targets seemed to preferentially increase sensitivity to radiation in CREBBP/EP300 mutant tumors (Fig. 2C-E). Specifically, inhibition of the CREBBP and EP300 genes themselves, as well as the dual specificity protein kinase (TTK) were associated with increased *in vivo* sensitivity to radiation in the CREBBP/EP300 mutant but not wt tumors in the screen.

Inhibition of CREBBP or EP300 expression leads to in vitro radiosensitization, but only in the context of its cognate mutation.

We performed targeted knockdown (KD) of CREBBP or EP300 using shRNA in HNSCC cell lines (Fig. 3 and Supplemental Fig. 1) of varying CREBBP/EP300 mutation status (Supplemental table 3). These cell lines were then treated with radiation and clonogenic survival was assayed (Fig. 2F). CREBBP or EP300 KD was associated with increased sensitivity to radiation, but only in the context of a mutation in the cognate

gene. For example, CREBBP KD, but not EP300, led to significant radiosensitization in the CREBBP mutant cell line UM-SCC-22a, which is EP300 wt. Similarly, EP300 KD, but not CREBBP, led to significant radiosensitization in the EP300 mutant cell line UMSCC25 that is wt for CREBBP. This pattern was consistently observed over all cell lines tested (Fig. 2F).

CREBBP inhibition leads to mutation specific apoptosis and decreased DNA damage repair following radiation.

We next examined apoptosis in CREBBP KD cell lines (Fig. 3A & B). The combination of CREBBP inhibition and radiation led to dramatically increased TUNEL staining and caspase 3 cleavage in CREBBP mutant (but not wt) cell lines (Fig. 3A & B). We also examined the DNA damage response via immunofluorescence staining of DNA damage foci (Fig. 3C). Interestingly, the induction of γ-H2AX was greater in CREBBP inhibited cell lines that harbored CREBBP mutations, but not those harboring wt CREBBP (Fig. 3C). Conversely, BRCA1 foci induction was significantly reduced following radiation in CREBBP inhibited cell lines in all the CREBBP mutant cell lines and HN30, which is both p53 and CREBBP wt (Fig. 3C). However, γ-H2AX induction was also less in HN30 following radiation in CREBBP KD. Irrespective of mutational status, inhibition of CREBBP generally had little effect on 53BP1 foci formation following radiation (Fig. 3C).

CREBBP inhibition leads to in vivo radiosensitization.

We further evaluated the therapeutic potential of targeting CREBBP using two separate *in vivo* models of CREBBP mutant HNSCC. We initially used the CREBBP mutant cell line UM-SCC-47 to generate tumors in the mouse flank and treated with 2

Gy x 8 days. Radiation or CREBBP KD (using two distinct shRNA constructs) alone had minimal to modest effect, however the combination led to a profound tumor growth delay and improved survival (Fig. 4A & B). Indeed, at the conclusion of the tumor growth delay experiment 5 tumors in the irradiated shCREBBP-2 group (45%) and 7 tumors in the irradiated shCREBBP-3 group (64%) had regressed below the limits of detection. An separate TUNEL staining study showed increased apoptosis in the shCREBBP + radiation tumors compared to other groups (Fig. 4C). We performed a similar experiment using tumors derived from CREBBP mutant UM-SCC-22a cells (Fig. 4D). While inhibition of CREBBP alone had a significant effect in this model, we again observed a profound radiosensitization, with nearly all the irradiated tumors in both CREBBP knockdown groups regressing below the limits of detection.

The observed synthetic cytotoxicity is not solely CREBBP or EP300 expression level dependent.

One potential explanation for the observed synthetic cytotoxicity is a dose-dependency. Namely, if basal levels of CREBBP or EP300 are significantly diminished in mutant cells, the observed effect may simply be due to a more complete inhibition of the protein. To explore this hypothesis, we examined basal expression in HNSCC cell lines and tumors in the context of various CREBBP and EP300 mutations. Interestingly, basal CREBBP and EP300 gene expression in the cell lines used in this study were not directly associated with underlying mutation (Supplemental Fig. 2A). Moreover, in a panel of 82 HNSCC cell lines, neither CREBBP nor EP300 mutation was directly associated with mRNA expression (Supplemental Fig. 2B). In the TCGA HNSCC cohort, no significant difference in CREBBP or EP300 gene expression was observed in mutant

tumors (Supplemental Fig. 2C). Similarly, neither CBP or p300 protein were associated with mutation in the cell lines used in this study (Supplemental Fig. 2D & E). Moreover, even in the context of nearly complete inhibition of CREBBP protein expression (Fig. 3 & Supplemental Fig. 1) neither HN31 nor HN30 (CREBBP wt cell lines) were sensitized to radiation (Fig. 2). Conversely, incomplete inhibition of EP300 (in the case of EP300 mutants HN5 and HN30) led to significant radiosensitization (Fig. 2, Fig. 3 & Supplemental Fig. 1).

Inhibition of CBP and p300 histone acetyltransferase (HAT), but not bromodomain function, leads to synthetic cytotoxicity.

We next examined chemical inhibitors of CREBBP and/or EP300 function: 1) ICG-001, a CBP specific inhibitor that is thought to inhibit the interaction between CBP and β-catenin, although it is also known to have β-catenin independent effects (note: PRI-724 is an active enantiomer of ICG-001); 2) GNE-272, a bromodomain specific inhibitor for both CREBBP and EP300; 3) A-485, a histone acetyltransferase inhibitor specific for CREBBP and EP300 (A-486 is an inactive analog and used as a negative control).

ICG-001 led to significant *in vitro* radiosensitization on clonogenic assay, but only in those cell lines harboring a CREBBP mutation (Fig. 5A-D). This effect was largely due to increased apoptosis following the addition of ICG-001 to radiation (Fig. 5E). Although the enantiomer of ICG-001, PRI-724, is actively in clinical trial development, neither of these agents target p300, and as predicted, we did not observe synthetic cytotoxicity in a CREBBP wt or an EP300 mutant cell line (Fig 5C & D).

To maximize the clinical impact of the observed synthetic cytotoxicity we utilized additional inhibitors, currently in clinical development, that inhibit both CBP and p300 function. We initially tested GNE-272, a bromodomain inhibitor, however this agent had no effects on sensitivity to radiation on clonogenic assay (Supplemental Fig. 3), independent of CREBBP or EP300 status. However, the HAT inhibitor A-485, but not inactive A-486 analog, led to radiosensitization in cell lines harboring a mutation in either CREBBP or EP300 (Fig. 6A), but not in wt cell lines (Fig. 6B). The observed radiosensitization was largely due to increased apoptosis following the combination of A-485 and radiation (Fig. 6C & D).

Discussion

To identify mutations associated with poor response that can be utilized to generate synthetic cytotoxicity, we have performed, to our knowledge, one of the largest analyses of an irradiated head and neck patient population, examining all genes mutated in the malignancy with sufficient frequency to be considered as potential prognostic markers. Two analyses were performed, both in the larger group of patients in the TCGA cohort who received radiation, as well as a subset analysis of patients with known treatment and patterns of failure.

In the initial analysis, mutations in TP53 were associated with worse outcome in this study. Our group and others have linked TP53 mutation with outcome in HNSCC in a variety of contexts (1,13–15). However, in the more homogenous population this association was lost, which is also consistent with our previous data which indicate that TP53 must be stratified by function to be predictive (1).

Three additional and unexpected genes emerged from this analysis, specifically CASP8 and the CBP-p300 coactivator family (CREBBP and EP300), mutations in all of which were associated with dramatically higher rates of treatment failure. This may not be surprising in the case of CASP8, as this gene is intimately involved in apoptosis and one might conclude that a simple blocking of apoptosis is the sole explanation of this phenomenon. However, the response of most solid epithelial tumors to conventional radiation is not classical apoptosis, but rather alternative modes of cell death, most prominently mitotic catastrophe (16,17). Thus, deficient apoptosis in this setting may be an insufficient explanation of this phenomenon and further study is necessary.

Mutations in the related histone acetyltransferases, CREBBP and EP300, were also associated with treatment failure following radiation. The relationship between mutation in CREBBP or EP300, inhibition of CREBBP or EP300, and treatment with DNA damaging agents is understudied. CREBBP and EP300 are homologous multifunctional bromodomain-containing acetyltransferases that can regulate many proteins and pathways. They have significantly overlapping functions, and many chemical inhibitors under development for clinical use target both with approximately equal efficacy (8, 11). Taken together, CREBBP and EP300 are collectively mutated in 13% of HNSCC and 14% of all squamous cancers (5, 6), with similar frequencies in both HPV positive and HPV negative disease. Missense mutations are clustered in the acetyltransferase domain, and there is a reasonable frequency of truncating mutations (~20%). We have observed a similar pattern of mutations in our panel of HNSCC cell lines. Additionally, many of these mutations are heterozygous, indicating possible haploinsufficiency, as has been seen for the chromatin modifying genes in the BAF

complex (19). Although these genes are mutated in HNSCC they have not been extensively studied in this tumor type and further study is necessary in regard to their effect on tumorigenesis in HNSCC.

In this study we have linked clinical data with *in vivo* screening, informed by the knowledge that significant context is lost utilizing *in vitro* screening analyses. Thus, we performed *in vivo* shRNA screening focused upon DNA damage repair and targetable proteins. Once completed, these screens were analyzed in the context of either CASP8 or CREBBP/EP300 mutations, searching for synthetically cytotoxic combinations with radiation. Although we did not observe synthetically cytotoxic targets in CASP8 tumors, we identified several in the CREBBP/EP300 mutant tumors, including the CREBBP and EP300 genes themselves. Due to these observations, and the availability of agents targeting CREBBP and EP300 already under clinical investigation, we selected them for further validation.

Both *in vitro* and *in vivo*, we observed a similar phenomenon, namely that inhibition of either gene individually led to a dramatic sensitization to radiation, but only in the context of their cognate mutation. The effect was associated with both increased induction of DNA damage following radiation as well as inhibition of homologous recombination (HR), leading to increased early apoptosis. This latter effect is interesting in that most HNSCC cell lines and tumors are relatively resistant to apoptosis following DNA-damaging therapies, such as radiation or chemotherapy (1,17–20). Thus, this phenotype represents an unexpected but important shift in response.

We further examined the therapeutic relevance of these findings by using inhibitors of specific CREBBP or EP300 functions in combination with radiation. While

bromodomain inhibitors exhibited no synthetic cytotoxicity, the use of HAT inhibitor exhibited dramatic sensitization to radiation, but only in the context of a mutation in either CREBBP or EP300. This points towards the histone acetylase function of either protein to be critical for the observed phenomenon. Indeed, inhibition of key histone marks was observed only in mutant cells that exhibited synthetic cytotoxicity.

We have seen that the combination of HAT inhibition and DNA damage leads to a synthetic cytotoxicity in tumors harboring mutations in the CBP-p300 coactivator family. The mechanism of this phenomenon is likely complex. The most well-characterized functions for CBP and p300 are as protein acetyltransferases. The primary targets of this acetylation are histone tails (H3K18, H3K27, H4K5/8/12/16) where they function to open the chromatin structure and facilitate gene expression. The dysfunction of either of these proteins leads to a loss of histone acetylation, a process that can affect DNA damage repair. Firstly, inhibition of CBP and p300 can transcriptionally repress BRCA1 via a lack of histone acetylation of that gene's promoter region and binding E2F1 (21). In that study, genes associated with non-homologous end joining (NHEJ) were not associated with CBP/p300 modulation. We observed similar results in our own model, with the predominant effect appearing to be on HR. However, additional studies have linked CBP/p300 modulation of histone acetylation directly to both alterations of NHEJ or HR depending upon the study and cellular context (22–24). Thus, effects on DDR may be largely context dependent, varying with genetic background as well as with specific genetic insult.

As stated, the synthetic cytotoxicity observed in this study is dependent upon mutations in the CBP-p300 coactivator family. The reasons for this are likely several-

fold. Firstly, cell lines and tumors expressing mutations, particularly truncating mutations, in these genes potentially lead to less protein product. Thus, the phenomenon could be a simple dosing effect. However, we presented several lines of evidence suggest that this may be an incomplete explanation. Firstly, basal expression of either CREBBP or EP300 were not directly correlated with mutations in cell lines or tumors. Moreover, degree of inhibition of either CREBBP or EP300 was overridden by mutational status as a predictor of response. It has been proposed that CREBBP/EP300 mutations in some non-HNSCC cell lines confer a gain of function (25). These mutations were described to truncate the protein after the HAT domain, although this specific pattern of mutation is not common in HNSCC mutations. Further studies will need to be performed to determine the exact relationship between mutation, expression and synthetic cytotoxicity in this disease.

In conclusion, we have both identified novel prognostic markers of treatment failure in HNSCC as well as explored a novel synthetic cytotoxicity involving one of these biomarkers, mutated CREBBP/EP300. This synthetic cytotoxicity appears to specifically involve effects on DNA damage repair, rendering HR deficient following DNA damage and leading to increased apoptosis. Moreover, this effect can be created using a HAT inhibitor which is currently being explored for clinical trial use, and thus could be translated clinically to improve outcomes in this deadly disease.

References

1. Skinner HD, Sandulache VC, Ow TJ, Meyn RE, Yordy JS, Beadle BM, et al. TP53 disruptive mutations lead to head and neck cancer treatment failure through inhibition of radiation-induced senescence. Clin Cancer Res Off J Am Assoc Cancer Res. 2012;18:290–300.

2. Hess J, Unger K, Maihoefer C, Schüttrumpf L, Wintergerst L, Heider T, et al. A Five-MicroRNA Signature Predicts Survival and Disease Control of Patients with Head and Neck Cancer Negative for HPV Infection. Clin Cancer Res. 2019;25:1505–16.

3. Theodoraki M-N, Yerneni SS, Hoffmann TK, Gooding WE, Whiteside TL. Clinical Significance of PD-L1+ Exosomes in Plasma of Head and Neck Cancer Patients. Clin Cancer Res Off J Am Assoc Cancer Res. 2018;24:896–905.

4. Liu X, Kumar M, Yang L, Molkentine DP, Valdecanas D, Yu S, et al. BAP1 Is a Novel Target in HPV-Negative Head and Neck Cancer. Clin Cancer Res Off J Am Assoc Cancer Res. 2018;24:600–7.

5. Kang H, Kiess A, Chung CH. Emerging biomarkers in head and neck cancer in the era of genomics. Nat Rev Clin Oncol. 2015;12:11–26.

6. Fong PC, Boss DS, Yap TA, Tutt A, Wu P, Mergui-Roelvink M, et al. Inhibition of poly(ADP-ribose) polymerase in tumors from BRCA mutation carriers. N Engl J Med. 2009;361:123–34.

7. Huang A, Garraway LA, Ashworth A, Weber B. Synthetic lethality as an engine for cancer drug target discovery. Nat Rev Drug Discov. 2020;19:23–38.

8. Gillet J-P, Varma S, Gottesman MM. The Clinical Relevance of Cancer Cell Lines. JNCI J Natl Cancer Inst. 2013;105:452–8.

9. Katt ME, Placone AL, Wong AD, Xu ZS, Searson PC. In Vitro Tumor Models: Advantages, Disadvantages, Variables, and Selecting the Right Platform. Front Bioeng Biotechnol [Internet]. 2016 [cited 2019 Oct 15];4. Available from: https://www.frontiersin.org/articles/10.3389/fbioe.2016.00012/full

10. Campbell JD, Yau C, Bowlby R, Liu Y, Brennan K, Fan H, et al. Genomic, Pathway Network, and Immunologic Features Distinguishing Squamous Carcinomas. Cell Rep. 2018;23:194-212.e6.

11. Cancer Genome Atlas Network. Comprehensive genomic characterization of head and neck squamous cell carcinomas. Nature. 2015;517:576–82.

12. Carugo A, Genovese G, Seth S, Nezi L, Rose JL, Bossi D, et al. In Vivo Functional Platform Targeting Patient-Derived Xenografts Identifies WDR5-Myc Association as a Critical Determinant of Pancreatic Cancer. Cell Rep. 2016;16:133–47.

13. Poeta ML, Manola J, Goldwasser MA, Forastiere A, Benoit N, Califano JA, et al. TP53 mutations and survival in squamous-cell carcinoma of the head and neck. N Engl J Med. 2007;357:2552–61.

14. Osman AA, Neskey DM, Katsonis P, Patel AA, Ward AM, Hsu T-K, et al. Evolutionary Action Score of TP53 Coding Variants Is Predictive of Platinum Response in Head and Neck Cancer Patients. Cancer Res. 2015;75:1205–15.

15. Neskey DM, Osman AA, Ow TJ, Katsonis P, McDonald T, Hicks SC, et al. Evolutionary Action Score of TP53 Identifies High-Risk Mutations Associated with Decreased Survival and Increased Distant Metastases in Head and Neck Cancer. Cancer Res. 2015;75:1527–36.

16. Eriksson D, Stigbrand T. Radiation-induced cell death mechanisms. Tumour Biol J Int Soc Oncodevelopmental Biol Med. 2010;31:363–72.

17. Roninson IB, Broude EV, Chang BD. If not apoptosis, then what? Treatment-induced senescence and mitotic catastrophe in tumor cells. Drug Resist Updat Rev Comment Antimicrob Anticancer Chemother. 2001;4:303–13.

18. Prokhorova EA, Egorshina AY, Zhivotovsky B, Kopeina GS. The DNA-damage response and nuclear events as regulators of nonapoptotic forms of cell death. Oncogene. 2019;1–16.

19. Osman AA, Monroe MM, Ortega Alves MV, Patel AA, Katsonis P, Fitzgerald AL, et al. Wee-1 kinase inhibition overcomes cisplatin resistance associated with high-risk TP53 mutations in head and neck cancer through mitotic arrest followed by senescence. Mol Cancer Ther. 2015;14:608–19.

20. Gadhikar MA, Sciuto MR, Alves MVO, Pickering CR, Osman AA, Neskey DM, et al. Chk1/2 inhibition overcomes the cisplatin resistance of head and neck cancer cells secondary to the loss of functional p53. Mol Cancer Ther. 2013;12:1860–73.

21. Ogiwara H, Kohno T. CBP and p300 Histone Acetyltransferases Contribute to Homologous Recombination by Transcriptionally Activating the BRCA1 and RAD51 Genes. PLOS ONE. 2012;7:e52810.

22. Ogiwara H, Ui A, Otsuka A, Satoh H, Yokomi I, Nakajima S, et al. Histone acetylation by CBP and p300 at double-strand break sites facilitates SWI/SNF chromatin remodeling and the recruitment of non-homologous end joining factors. Oncogene. 2011;30:2135–46.

23. Tamburini BA, Tyler JK. Localized Histone Acetylation and Deacetylation Triggered by the Homologous Recombination Pathway of Double-Strand DNA Repair. Mol Cell Biol. 2005;25:4903–13.

24. Qi W, Chen H, Xiao T, Wang R, Li T, Han L, et al. Acetyltransferase p300 collaborates with chromodomain helicase DNA-binding protein 4 (CHD4) to facilitate DNA double-strand break repair. Mutagenesis. 2016;31:193–203.

25. Ghandi M, Huang FW, Jané-Valbuena J, Kryukov GV, Lo CC, McDonald ER, et al. Next-generation characterization of the Cancer Cell Line Encyclopedia. Nature. 2019;569:503–8.

Figure Legend

Figure 1. Whole exome sequencing identifies CASP8 and CREBBP/EP300 mutation significantly associated with treatment failure in HNSCC. A) Forrest plot of hazard ratios (HR) for Overall survival (OS) for TCGA patients known to have received radiation therapy. B & C) Forrest plot of HR for OS (B) & loco-regional recurrence (LRR) (C) in a subset of TCGA patients treated uniformly with surgery and radiation and known patterns of failure. B & C) Kaplan-Meier curves for LRR in patients with either CASP8 (D) or CREBBP/EP300 (E) mutations.

Figure 2. *In vivo* shRNA screening identifies synthetic cytotoxicity CREBBP/EP300 mutated tumors. A) Plot of RSA log p-values from control or irradiated tumors from the *in vivo* shRNA study. Targets below and to the left of the blue dashed line were selected for further examination as potential targets for synthetic cytotoxicity in combination with radiation. B & C) Ratio of CASP8 (B) or CREBBP/EP300 (C) mutant vs. wt for target fold change (y-axis) and RSA log p-value (x-axis) for targets selected from (A). D & E) Difference between CREBBP/EP300 mutant and wt tumors from the *in vivo* shRNA study in (C) as a function of target fold change (D) and RSA log p-value (E). F) Clonogenic assays following irradiation of HNSCC cell lines expressing control and either CREBBP or EP300 shRNA. In D & E, comparisons were evaluated using ANOVA with post-hoc Tukey's t-test. In F, each point for each group was compared to control using Student's t-test. For * - shCREBBP-2 and # - shCREBBP-3, $p<0.05$. All p-values two sided.

Figure 3. CBP-p300 coactivator mediated synthetic cytotoxicity results in impaired HR and increased apoptosis. A & B) Tunel staining (A) and caspase 3

immunoblot (B) following irradiation in HNSCC cells expressing control or CREBBP shRNA. (C) ɣ-H2AX, 53BP1, and BRCA1 foci following irradiation in shControl or shCREBBP HNSCC cells. Significance tested via students t-test. For A, * indicates a two-sided p<0.05 compared to the Control XRT group. For B & C two sided p-values are indicated.

Figure 4. CBP-p300 coactivator mediated synthetic cytotoxicity is observed in multiple *in vivo* HNSCC models. A & B) Tumor growth delay (A) and survival (B) in a UM-SCC-47 xenograft model expressing either control or two different CREBBP shRNAs following irradiation at 2 Gy/day for 5 days. C) *In vivo* TUNEL staining from UM-SCC-47 xenograft tumors collected 8h following the final dose of radiation in a concurrent experiment with (A). C) A similar experiment performed in the UM-SCC-22a xenograft model. For both models, the slope of the linear regression for both irradiated CREBBP KD groups was significantly different from other groups with at least a two-sided p<0.01. In B, log rank statistics comparing shCREBBP-2 XRT or sh-CREBBP-3 XRT groups compared to Control XRT showed a significant increase in survival (two-sided p<0.05) in both groups.

Figure 5. ICG 001 produces synthetic cytotoxicity in CREBBP mutant HNSCC cell lines. A-D) Clonogenic survival following irradiation and ICG-001 in CREBBP mutant (A & B) and wt (C & D) cell lines. E) Tunel assay following the same combination (p-values are two-sided and derived from Student's t-test). Clonogenic survival curves analyzed as in Figure 2.

Figure 6. The HAT inhibitor A485 exhibits synthetic cytotoxicity and inhibition of several histone marks in HNSCC cells with mutations in the CBP-p300 co-

activator family. A & B) Clonogenic survival following irradiation and either A485 (active) or A486 (inactive) in CREBBP/EP300 mutant (A) or wt (B) HNSCC cells. Clonogenic survival curves analyzed as in Figure 2. C) TUNEL assay in UM-SCC-47 (CREBBP mut), HN5 (CREBBP/EP300 mut) and HN31 (CREBBP/EP300 wt) cells treated with irradiation and either A485 (active) or A486 (inactive) (p-values are two-sided and derived from Student's t-test). D) Immunoblot for cleaved caspase 3 in the indicated treatment groups.
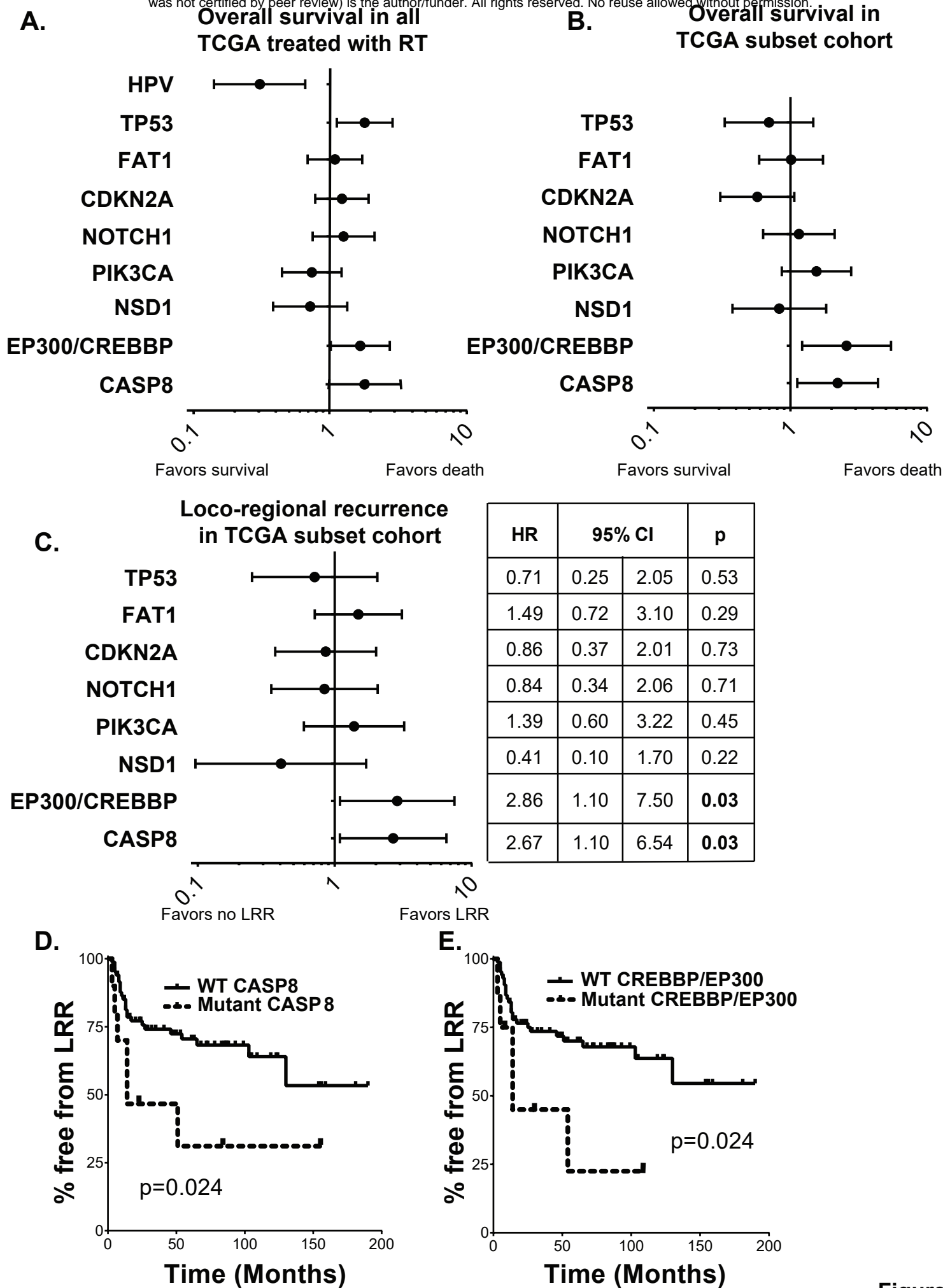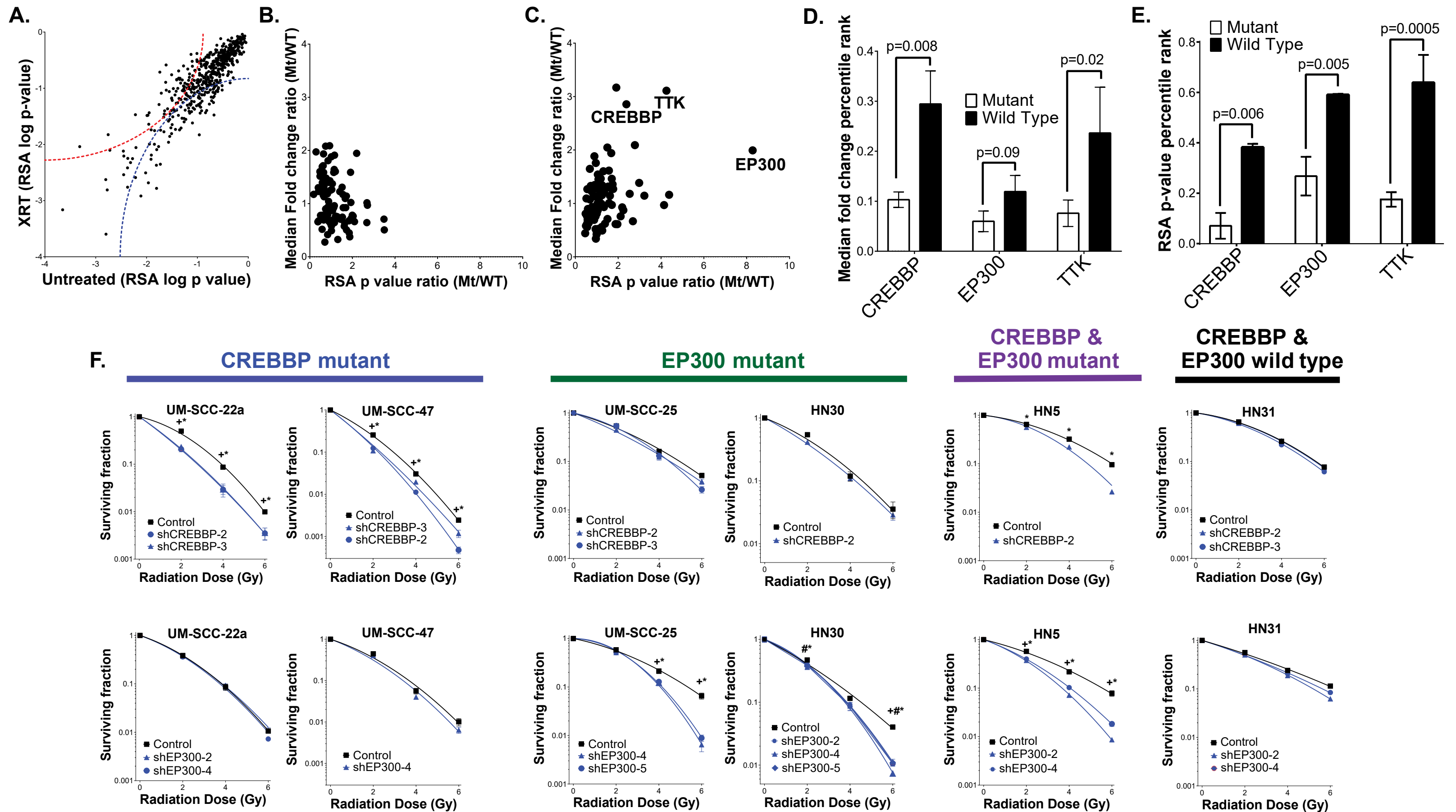
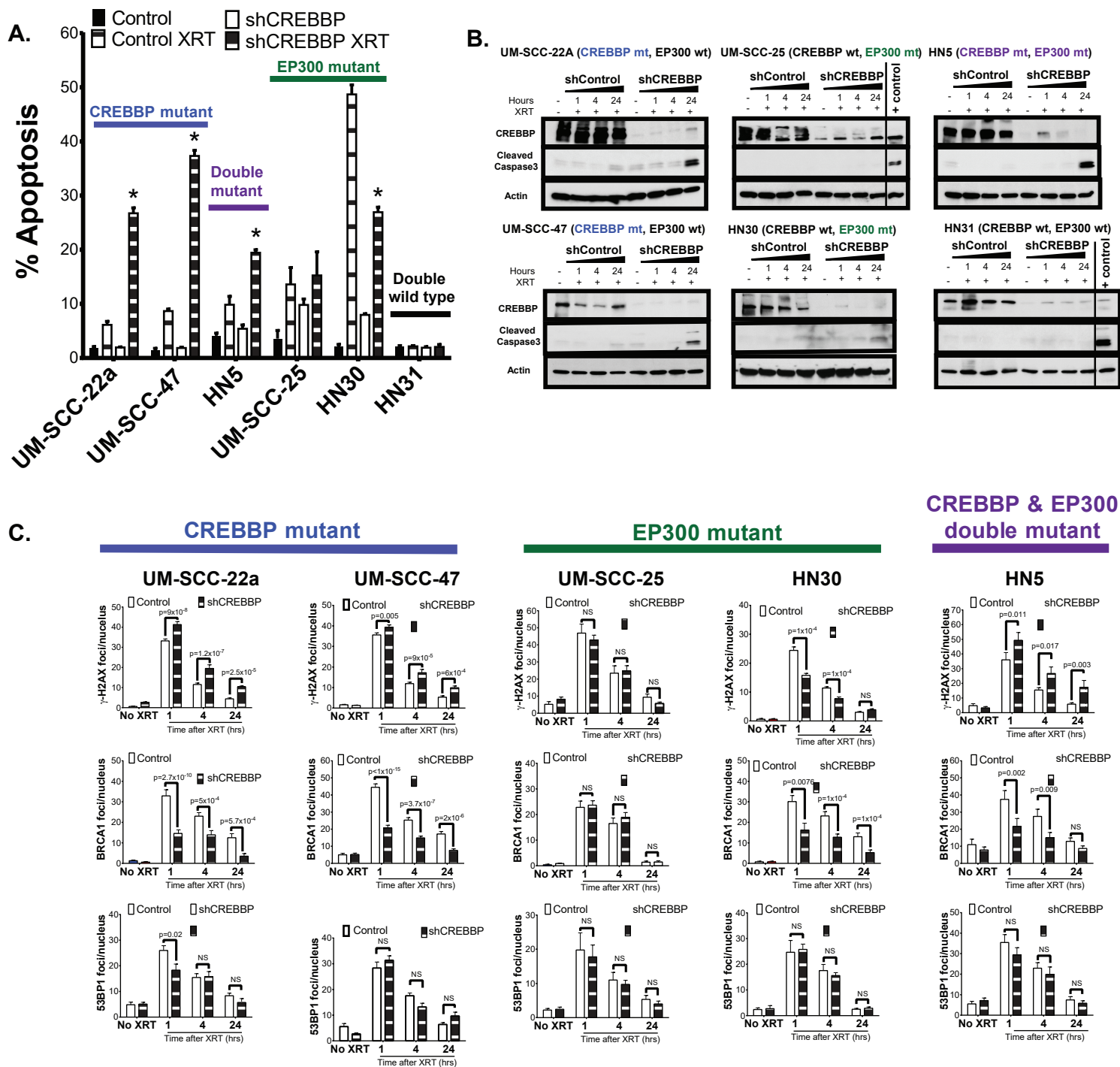**A.** **Overall survival in all TCGA treated with RT**

B. **Overall survival in TCGA subset cohort**

C. **Loco-regional recurrence in TCGA subset cohort**

HR	95% CI		p
0.71	0.25	2.05	0.53
1.49	0.72	3.10	0.29
0.86	0.37	2.01	0.73
0.84	0.34	2.06	0.71
1.39	0.60	3.22	0.45
0.41	0.10	1.70	0.22
2.86	1.10	7.50	**0.03**
2.67	1.10	6.54	**0.03**

D.

WT CASP8
Mutant CASP8

p=0.024

E.

WT CREBBP/EP300
Mutant CREBBP/EP300

p=0.024

Figure 1

Figure 2

Figure 3
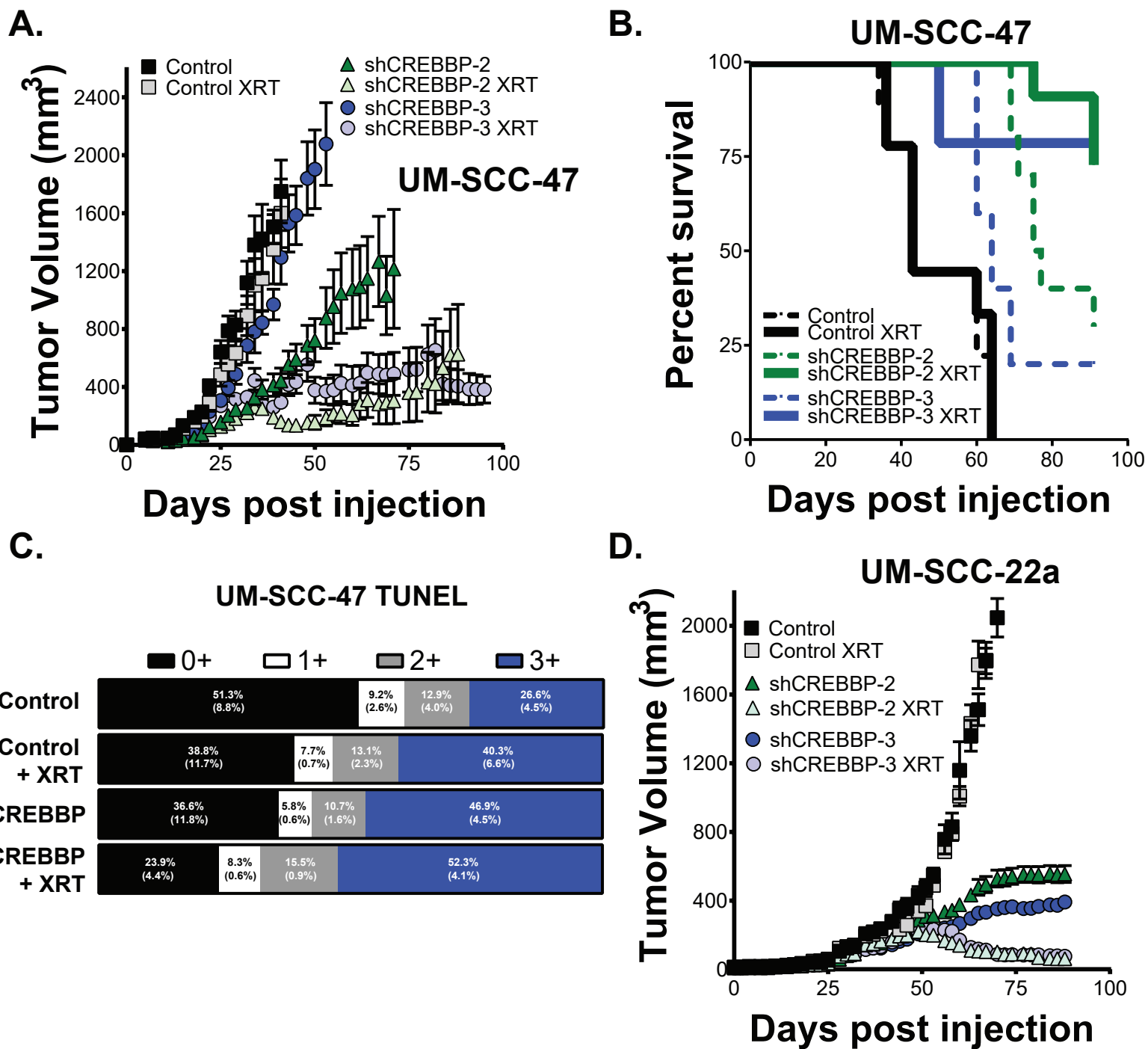
Figure 4

Figure 5

Figure 6